

Frequency-dependent tidal dissipation in a viscoelastic Saturnian core and expansion of Mimas' semi-major axis

D. Shoji and H. Hussmann

German Aerospace Center(DLR), Institute of Planetary Research, Rutherfordstr. 2 12489 Berlin, Germany

e-mail: [Daigo.Shoji; Hauke.Hussmann]@dlr.de

Received ; accepted

ABSTRACT

Context. Regarding dissipation in Saturn, usually parameterized by Saturn's quality factor Q , there remains a discrepancy between conventional estimates and the latest determination that has been derived from astrometric observations of Saturn's inner satellites. If dissipation in Saturn is as large as the astrometric observations suggest, Mimas would migrate fast due to tidal torques exerted by Saturn. In that case its initial orbital would be located inside the synchronous orbit or even inside Saturn's Roche-limit contradicting orbital evolution models.

Aims. Using simple structure models and assuming Saturn's core to be viscoelastic, we suggest dissipation models which are consistent with both the latest observations and with Mimas' orbital migration.

Methods. We calculated the ranges of rigidity and viscosity which are consistent with the observed Saturnian dissipation. Within the constrained rheological parameters, Mimas' initial semi-major axis was calculated considering the frequency dependence of dissipation in Saturn's core.

Results. If the viscosity of the solid core is near the lower boundary to generate the observed dissipation ($k_{2s}/Q_s \sim 4 \times 10^{-5}$), Mimas can stay outside the synchronous orbit and the Roche limit for 4.5 billion years of evolution, and Saturnian Q becomes less than 10^4 .

Conclusions. In the case of a frequency dependent viscoelastic dissipative core, the lower boundary of the observed Saturnian dissipation can be consistent with the orbital expansion of Mimas. In this model, the assumption of a late formation of Mimas, discussed recently, is not required.

Key words. planets and satellites: interiors– planets and satellites: individual: Saturn – planets and satellites: individual: Mimas

1. Introduction

Tidal dissipation in Saturn induced by its moons can be one important factor to consider the interior structure and dynamics of Saturn. The magnitude of dissipation is estimated by the quality factor, Q , which is defined as the ratio between the peak of the stored energy and the dissipated energy by one cyclic force. Small Q value means that a large magnitude of energy is dissipated in Saturn.

Although the Saturnian Q value is not constrained well, the minimum value of Saturnian Q has been evaluated by the orbital expansion of Mimas (e.g. Goldreich & Soter 1966; Gavrilov & Zharkov 1977; Murray & Dermott 2000). The tidal bulge on Saturn by Mimas is ahead of the Saturn-Mimas axis because Saturn's rotation period is smaller than the orbital period of Mimas. This tidal bulge adds a torque to Mimas and the semi-major axis of Mimas increases. Increasing rate of semi-major axis a of Mimas is given (e.g., Murray & Dermott 2000) by

$$\frac{da}{dt} = 3 \sqrt{\frac{G}{M_s}} \frac{M_m R_s^5}{a^{5.5}} \frac{k_{2s}}{Q_s}, \quad (1)$$

where t , G , M_s , M_m and R_s are time, the gravitational constant, Saturnian mass, Mimas' mass and Saturnian radius, respectively. k_{2s} and Q_s are the second order of Love number and the Q value of Saturn. By integrating Eq. (1) backward in time, the past semi-major axis of Mimas can be calculated. As this equation shows, the change of the orbit becomes large when Q_s is small. In order to move to the current orbit from a small initial semi-major axis in the past, Mimas must be located outside of the surface (and the Roche limit) of Saturn when it was formed. Assuming constant $Q_s < 10^4$ and reasonable values of $k_{2s}=0.341$ (Gavrilov & Zharkov 1977), Mimas moves from the Saturnian surface to the current position within much less than the solar system age (~ 4.5 Ga). If we assume that the age of Mimas is almost the same as the solar system age, expansion of orbit must be slower. Thus, at least a few tens of thousand of Q_s is required (e.g. Goldreich & Soter 1966; Gavrilov & Zharkov 1977; Murray & Dermott 2000). Meyer & Wisdom (2007) indicate that Mimas should be outside of the synchronous orbit where Mimas' orbital period is the same as the rotational period of Saturn because the orbit of Mimas does not expand inside of the synchronous orbit. Their evaluation also suggests that the Saturnian Q is more than 18,000 (Murray & Dermott 2000), which is compatible with other studies (e.g. Goldreich & Soter 1966; Gavrilov & Zharkov 1977; Murray & Dermott 2000).

However, recent measurements of Saturnian dissipation have indicated that the Q value of Saturn is a few thousand only (Lainey et al. 2012, 2017). As a mechanism of the observed dissipation of Saturn, Lainey et al. (2017) suggest viscoelastic response of the solid core. Although a viscoelastic core can generate significant dissipation (Remus et al. 2012, 2015; Lainey et al. 2017), it contradicts the conventional estimations derived from the orbital expansion of Mimas (Goldreich & Soter 1966; Gavrilov & Zharkov 1977; Murray & Dermott 2000). One hypothesis is that the Saturnian satellites such as Mimas were formed recently (Charnoz et al. 2011). If Mimas moved

to the current position with a small time scale, large dissipation of Saturn does not contradict the orbital expansion of Mimas.

Dissipation of Saturn plays an important role in the activity of the Saturnian satellite as well as Saturn itself. The Cassini probe has observed that Enceladus is a current active body emanating water plumes, possibly implying liquid water in its subsurface (e.g. Porco et al. 2006). Although one of the main heat sources to maintain the subsurface ocean should be tidal heating of Enceladus by its elliptical orbit, the detailed mechanism to maintain the ocean by tides is not known well so far. If Enceladus is in equilibrium state of the resonance with Dione, the heating rate generated in Enceladus is ~ 1.1 GW at $Q_s=18,000$ (Meyer & Wisdom 2007), which is independent of the interior structure of Enceladus. However, the equilibrium heating rate increases with decreasing Q_s (Meyer & Wisdom 2007; Lainey et al. 2012), which may affect Enceladus' structure and activity.

Although the late formation of Mimas cannot be ruled out, in this work, we reconsider the conventional estimations derived from orbital migration of Mimas using a viscoelastic Saturnian core. In case of viscoelastic response, both Love number and Q value depend on frequency of cyclic forcing. Because the frequency of tide on Saturn changes with Mimas' semi-major axis, k_{2s} and Q_s in Eq. (1) cannot be constant. We calculate the past semi-major axis of Mimas taking into account the frequency dependence of the dissipation with the simple structure models by Remus et al. (2012, 2015). Firstly we constrain the rigidity and viscosity of the solid core which are consistent with the latest observational results by Lainey et al. (2017), and then we calculate the semi-major axis within the range of the constrained rheological parameters. By the two calculations, we suggest the Saturnian models which can be consistent with both Mimas' orbital evolution and the latest observational results of Saturnian dissipation.

2. Structure and rheology of Saturn

Remus et al. (2012, 2015) have explained the large dissipation of Saturn using the two layer model with fluid envelop and viscoelastic solid core. Here we assume this simple structure model because the purpose of this work is to relate the observed dissipation to Mimas' orbital change. Mass and size of Saturn are shown in Table 1, which are consistent with Remus et al. (2012, 2015). Lainey et al. (2017) assume more detailed models with layered structure and mention that the viscosity range to generate observed Q_s is compatible between their complex model and the simple two layer model. In the case of viscoelastic material, due to the delay of the response to forcing, Love number becomes complex \tilde{k}_{2s} , which is given (Remus et al. 2015) by

$$\tilde{k}_{2s} = \frac{3\tilde{\epsilon} + \frac{2}{3}\beta}{2\alpha\tilde{\epsilon} - \beta}, \quad (2)$$

where

$$\alpha = 1 + \frac{5}{2} \left(\frac{\rho_c}{\rho_o} - 1 \right) \left(\frac{R_c}{R_s} \right)^3 \quad (3)$$

$$\beta = \frac{3}{5} \left(\frac{R_c}{R_s} \right)^2 (\alpha - 1) \quad (4)$$

$$\tilde{\epsilon} = \frac{\frac{19\tilde{\mu}_c}{2\rho_c g_c R_c} + \frac{\rho_o}{\rho_c} \left(1 - \frac{\rho_o}{\rho_c} \right) \left(\beta + \frac{3}{2} \right) + \left(1 - \frac{\rho_o}{\rho_c} \right)}{\left(\alpha + \frac{3}{2} \right) \frac{\rho_o}{\rho_c} \left(1 - \frac{\rho_o}{\rho_c} \right)}. \quad (5)$$

R_c , g_c , ρ_c and ρ_o are radius of the core, gravitational acceleration at the surface of the core, density of the core and density of the envelop, respectively. We consider the value of R_c between $0.2R_s$ and $0.24R_s$, which includes the core radius by Remus et al. (2015). g_c , ρ_c and ρ_o can be calculated from the mass of the core M_c , R_s and R_c shown in Table 1. $\tilde{\mu}_c$ is the complex shear modulus of the viscoelastic core. In this work, we assume a Maxwell rheology in which the complex shear modulus of the Maxwell model is given by

$$\tilde{\mu}_c = \frac{\omega_f \mu \eta}{\omega_f \eta + i\mu}, \quad (6)$$

where $i = \sqrt{-1}$. μ and η are the tidally effective rigidity and viscosity of the solid core of Saturn. ω_f is the forcing frequency. For the frequency of tides on Saturn by satellites, ω_f can be represented by the rotational angular velocity of Saturn Ω and the mean motion of the satellites ω as $\omega_f = 2(\Omega - \omega)$. Because the Q value can be represented as $Q_s = |\text{Re}(\tilde{k}_{2s})/\text{Im}(\tilde{k}_{2s})|$ and the real part of Love number is much larger than the imaginary part ($k_{2s} \approx \text{Re}(\tilde{k}_{2s})$), k_{2s}/Q_s can be approximated by $|\text{Im}(\tilde{k}_{2s})|$.

Table 1. Physical parameters and values.

Parameter	Symbol	Value	Unit
Radius of Earth	R_\oplus	6.371×10^6	m
Mass of Earth	M_\oplus	5.9736×10^{24}	kg
Radius of Saturn	R_s	$9.14 R_\oplus$	
Mass of Saturn	M_s	$95.159 M_\oplus$	
Mass of solid core	M_c	$18.65 M_\oplus$	
Rotation rate of Saturn	Ω	1.65×10^{-4}	rad s ⁻¹
Mass of Mimas	M_m	3.7493×10^{19}	kg
Semi-major axis of Mimas	a_0	1.8552×10^8	m

3. Method

3.1. Constraint of rigidity and viscosity for observed dissipation

Firstly we calculate the ranges of rigidity and viscosity which are consistent with the observed k_{2s}/Q_s at the tidal frequency by Enceladus, Tethys and Dione. Although Lainey et al. (2017) also estimated k_{2s}/Q_s at Rhea's frequency, which is much larger than the frequency of the other three satellites, they suggest that the dissipation at Rhea's frequency is caused by turbulent friction in the envelope, which is beyond the scope of this work. k_{2s}/Q_s is $(20.70 \pm 19.91) \times 10^{-5}$, $(15.84 \pm 12.26) \times 10^{-5}$ and $(16.02 \pm 12.72) \times 10^{-5}$ at the tidal frequency of Enceladus, Tethys and Dione, respectively, and $(1.59 \pm 0.74) \times 10^{-4}$ in a global estimation (Lainey et al. 2017). Thus, we consider $|\text{Im}(\tilde{k}_{2s})|$ between 4×10^{-5} and 2.5×10^{-4} . k_{2s}/Q_s is almost independent of the mean motion difference among these three satellites (Lainey et al. 2017). We set $\omega_f = 2.5 \times 10^{-4} \text{ rad s}^{-1}$, which is between the tidal frequencies of Enceladus and Dione.

3.2. Change of Mimas' semi-major axis

As a next step, we calculate the initial semi-major axis of Mimas with the constrained rigidity and viscosity. Assuming a Kepler orbit, mean motion of Mimas is given by $\omega = \sqrt{GM_s/a^3}$. Substituting $|\text{Im}(\tilde{k}_{2s})|$ in Eq. (1), da/dt and dissipation of Saturn can be coupled by Eqs. (1)-(6). Integrations of a are performed backward from the current semi-major axis $a_0 = 1.8552 \times 10^8 \text{ m}$ (Murray & Dermott 2000) with a Runge-Kutta method and 10^4 yr of time step. We performed additional calculations with time step of 10^3 yr and $5 \times 10^2 \text{ yr}$ and the results did not change. For simplicity, the angular velocity of Saturn's rotation and the mass of Mimas are fixed at $\Omega = 1.65 \times 10^{-4} \text{ rad s}^{-1}$ (Giampieri et al. 2006; Anderson & Schubert 2007) and $M_m = 3.7493 \times 10^{19} \text{ kg}$ (Jacobson et al. 2006), respectively.

4. Results

4.1. Rigidity and viscosity ranges for observed dissipation

Fig. 1 shows $|\text{Im}(\tilde{k}_{2s})|$ as a function of rigidity and viscosity of Saturn's core. The rigidity and viscosity ranges which are consistent with the observed Saturnian dissipation (Fig. 2) are compatible with the rheological values estimated by Remus et al. (2015). $|\text{Im}(\tilde{k}_{2s})|$ becomes maximum at around 10^{15} Pa s . Although rigidity and viscosity which attain the observed $|\text{Im}(\tilde{k}_{2s})|$ change with the core radius, minimum viscosities for the observed dissipation should be 10^{13} - 10^{14} Pa s . If $\eta \sim 10^{15} \text{ Pa s}$, $|\text{Im}(\tilde{k}_{2s})|$ becomes too high to be consistent with the observed values.

4.2. Evolutions of dissipation and Mimas' orbit

Fig. 2 shows the evolutions of tidal frequency $2(\Omega - \omega)$, $|\text{Im}(\tilde{k}_{2s})|$ and semi-major axis a at $R_c = 0.219 R_s$. μ is $5 \times 10^{11} \text{ Pa}$ and $\eta = 5 \times 10^{13}$, 10^{14} and 10^{16} Pa s , which are consistent with the reasonable parameter range (Remus et al. 2015) and the observed k_{2s}/Q_s at the frequency of Enceladus, Tethys and Dione (Fig. 1). Due to the dissipation of Saturn, the semi-major axis decreases with decreasing

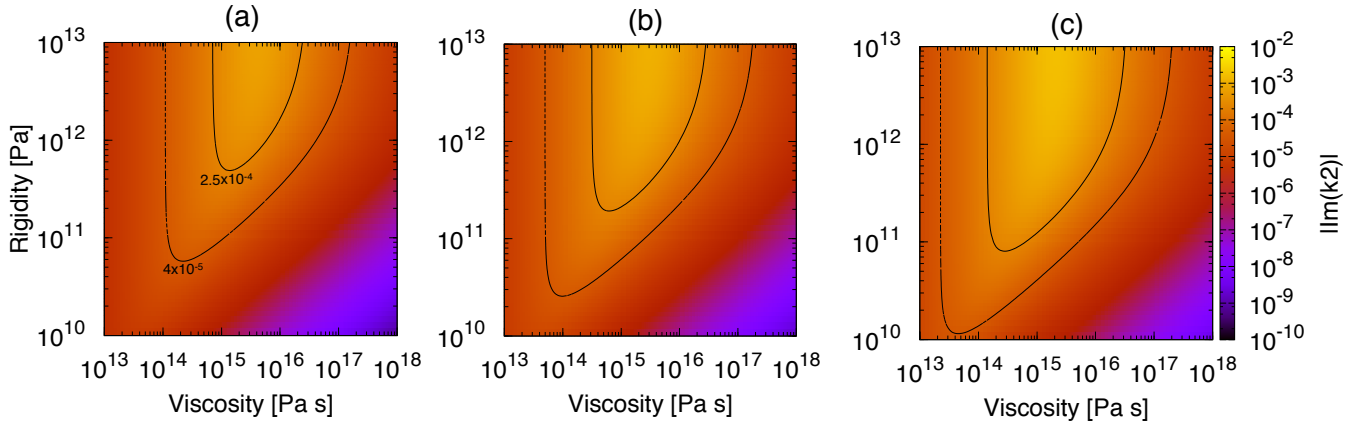


Fig. 1. $|\text{Im}(\tilde{k}_{2s})|$ as a function of viscosity and rigidity of the solid core. $\omega_f = 2.5 \times 10^{-4} \text{ rad s}^{-1}$ and the core radius is (a): $0.2R_s$ (b): $0.219R_s$ and (c): $0.24R_s$. Two contours show the upper $|\text{Im}(\tilde{k}_{2s})| = 2.5 \times 10^{-4}$ and the lower $|\text{Im}(\tilde{k}_{2s})| = 4 \times 10^{-5}$ boundaries which are consistent with the observed values.

time (Mimas' orbit expands with time). Because we assume $\omega = \sqrt{GM_s/a^3}$, $2(\Omega - \omega)$ also decreases as time decreases. However, once the semi-major axis decreases to the synchronous orbit with Saturn in which Mimas' orbital period is the same as the rotational period of Saturn ($\Omega = \omega$), dissipation does not occur because $2(\Omega - \omega)$ becomes zero, and thus the migration of Mimas stops. At $\eta = 5 \times 10^{13} \text{ Pa s}$ and 10^{14} Pa s , $|\text{Im}(\tilde{k}_{2s})|$ decreases with decreasing time (Fig. 2 b). In this viscosity range, $2(\Omega - \omega)/2\pi$ is smaller than the Maxwell frequency (μ/η). Thus the response of the solid core is like fluid as a decreases ($2(\Omega - \omega)$ decreases) and the core becomes less dissipative. On the other hand, at $\eta = 10^{16}$, $|\text{Im}(\tilde{k}_{2s})|$ increases with decreasing time because $2(\Omega - \omega)/2\pi$ is larger than the Maxwell frequency. By the decrease of $2(\Omega - \omega)$ (increase of ω), the response of the solid core becomes viscoelastic from elastic, which results in large dissipation. Due to the large dissipation, a falls to the synchronous orbit at around -0.5 Ga (Fig. 2 c).

One important result is that, at $\eta = 5 \times 10^{13} \text{ Pa s}$, $2(\Omega - \omega)$ does not become zero and thus a does not get into the synchronous orbit at the time of solar system formation (around -4.5 Ga). Thus, if the viscosity of Saturn is around $\eta = 5 \times 10^{13} \text{ Pa s}$, the latest observational dissipation at the frequency of Enceladus, Tethys and Dione does not contradict the conventional evaluations that Mimas must be outside of the surface of Saturn 4.5 billion years ago (e.g., Goldreich & Soter 1966; Gavrilov & Zharkov 1977; Murray & Dermott 2000). In addition to the synchronous orbit, Mimas should be outside of the Roche limit. Assuming that Mimas is a rigid and spherical body, the distance of the Roche limit $a_L = R_s(3\rho_s/\rho_m)^{1/3}$ (Murray & Dermott 2000) while $a_L = 2.456R_s(\rho_s/\rho_m)^{1/3}$ if Mimas is fluid (Chandrasekhar 1969), where ρ_s and ρ_m are density of Saturn and Mimas, respectively. Using the values of our model ($\rho_s = 687.3 \text{ kg m}^{-3}$) and the mean density of Mimas at $\rho_m = 1150 \text{ kg m}^{-3}$

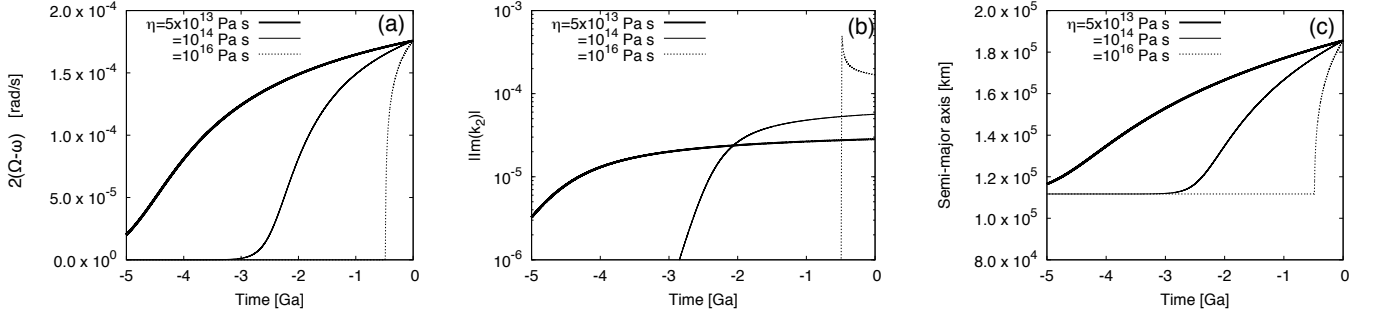


Fig. 2. Evolutions of (a): $2(\Omega - \omega)$ (b): $|\text{Im}(\tilde{k}_{2s})|$ and (c): a with different η at $R_c = 0.219R_s$ and $\mu = 5 \times 10^{11}$ Pa. Integrations are conducted backward in time and the current a of Mimas is shown at $t=0$.

(Thomas et al. 2007), $a_L \sim 7 \times 10^4$ km at the rigid Mimas and $\sim 1.2 \times 10^5$ km in the case of the fluid Mimas, respectively. Even if Mimas is a fluid body, it stays outside of the Roche limit at $\eta = 5 \times 10^{13}$ Pa s (Fig. 2).

We calculated Mimas' orbit with different rigidity within the consistent range to the observations. Although the magnitude of dissipation depends on rigidity, the value of viscosity strongly affects whether Mimas gets into the synchronous orbit because $|\text{Im}(\tilde{k}_{2s})|$ is relatively independent of rigidity at $\eta \sim 10^{13}$ - 10^{14} Pa s (Fig. 1). Thus, as long as the rigidity is consistent with the observations (Fig. 1), the conclusion that Mimas does not get into the synchronous orbit at lower boundary of the viscosity does not change.

In addition to low viscosity, the frequency dependence of $|\text{Im}(\tilde{k}_{2s})|$ is another reason why Mimas does not get into the synchronous orbit and the Roche limit. In the case of $\eta = 5 \times 10^{13}$ Pa s, $|\text{Im}(\tilde{k}_{2s})| = 2.8 \times 10^{-5}$ at $t=0$ (Fig. 2 b). Fig. 3 compares a of the case in which $|\text{Im}(\tilde{k}_{2s})|$ is fixed at 2.8×10^{-5} with the frequency dependent $|\text{Im}(\tilde{k}_{2s})|$ (coupled model of dissipation and orbit). While the semi-major axis is larger than the synchronous orbit for 4.5 billion years in the coupled model, Mimas' orbit becomes synchronous with Saturn at -3.5 Ga in the case of fixed $|\text{Im}(\tilde{k}_{2s})|$. As the semi-major axis decreases, due to the fluid response, $|\text{Im}(\tilde{k}_{2s})|$ decreases (Fig. 2 b) in the coupled model. Thus, da/dt becomes smaller as compared to the case with fixed $|\text{Im}(\tilde{k}_{2s})|$, which results in slow migration of Mimas.

Changes of semi-major axis at $R_c = 0.2R_s$ and $0.24R_s$ are shown in Fig. 4, respectively. Because the changing rate of the semi-major axis depends on $|\text{Im}(\tilde{k}_{2s})|$, Mimas can avoid getting into the synchronous orbit regardless of core radius if the viscosity of Saturn's core is a lower boundary for

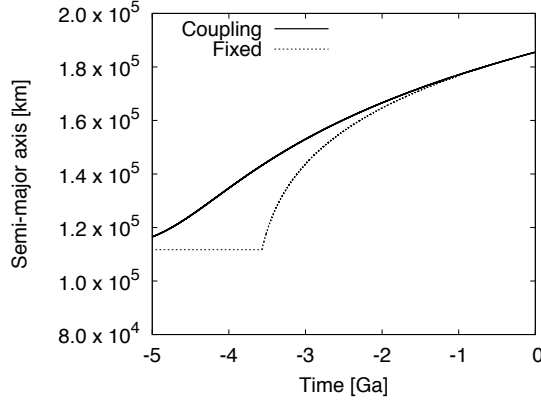


Fig. 3. Comparison of semi-major axis between constant $|\text{Im}(\tilde{k}_{2s})|$ at 2.8×10^{-5} and coupled orbital $|\text{Im}(\tilde{k}_{2s})|$ at $R_c = 0.219R_s$ and $\mu = 5 \times 10^{11}$ Pa. Once Mimas falls into the synchronous orbit, we assume that a does not change.

the observed k_{2s}/Q_s . It is uncertain that viscosity of Saturn's solid core can be in the order of 10^{13} Pa s. If 10^{14} Pa s of viscosity is required, Saturn should have small core at around $0.2R_s$.

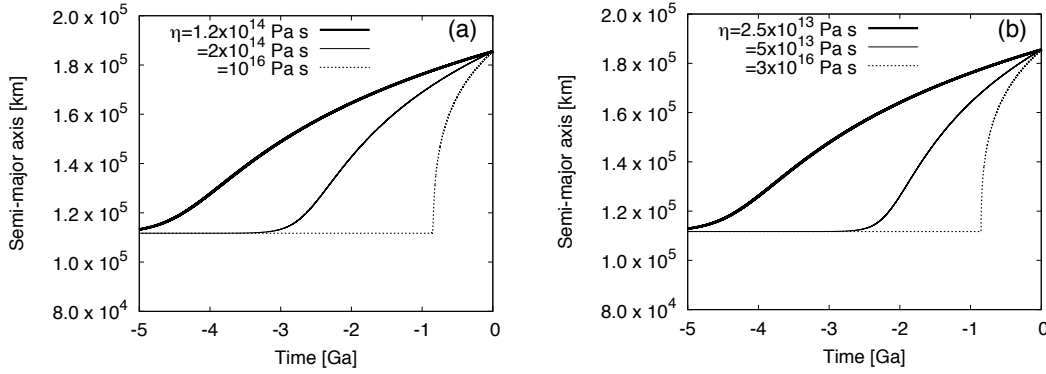


Fig. 4. Evolutions of semi-major axis at (a): $R_c = 0.2R_s$ and (b): $R_c = 0.24R_s$ and $\mu = 5 \times 10^{11}$ Pa and viscosities consistent with the observed dissipation.

One caveat of our results is that, although $\sim 4 \times 10^{-5}$ of $|\text{Im}(\tilde{k}_{2s})|$ is consistent with the observational values derived from each Saturnian satellite, it is smaller than the comprehensive evaluation at $|\text{Im}(\tilde{k}_{2s})| = (1.59 \pm 0.74) \times 10^{-4}$ (Lainey et al. 2017). Using the conventional ($k_{2s} = 0.341$) and the latest ($k_{2s} = 0.39$) values of the Saturnian Love number (Gavrilov & Zharkov 1977; Lainey et al. 2017), 4×10^{-5} of $|\text{Im}(\tilde{k}_{2s})|$ results in $Q_s = 8,525$ and $9,750$, respectively. Although these values are smaller than the conventional evaluations ($Q_s \gg 10^4$), they are still larger than the suggested value by Lainey et al. (2017) at $Q_s = 1,500$ – $2,500$. In the case of the simple two layer model, if $|\text{Im}(\tilde{k}_{2s})| \sim 8 \times 10^{-5}$, Mimas gets into the synchronous orbit from the current position ~ 3 billion years ago. Calculations with more accurate core structure may solve this discrepancy, which will be addressed in future studies.

5. Conclusions

Conventionally, the magnitude of Saturnian dissipation has been constrained from the orbital expansion of Mimas. Assuming constant Love number, more than a few tens of thousand of Saturnian Q is required for Mimas to stay outside of the surface of Saturn or the synchronous orbit 4.5 billion years ago (e.g. Goldreich & Soter 1966; Gavrilov & Zharkov 1977; Murray & Dermott 2000). However, the latest observations of Saturnian dissipation estimated at the orbital frequency of Enceladus, Tethys and Dione imply that the Saturnian Q is in the order of a few thousands, only (Lainey et al. 2017). We calculated the past semi-major axis of Mimas induced by tidal dissipation in Saturn's solid core assuming a Maxwell rheology and frequency dependence of k_{2s}/Q_s ($|\text{Im}(\tilde{k}_{2s})|$). If the viscosity of Saturn's core is consistent with the lower boundary of the observed dissipation ($k_{2s}/Q_s \sim 4 \times 10^{-5}$) (Lainey et al. 2017) and μ/η is larger than $2(\Omega-\omega)/2\pi$, due to the smaller tidal frequency in the past, Mimas can stay well outside the synchronous orbit even if it has formed 4.5 billion years ago. The viscosity consistent with the observations and Mimas' expansion changes with the radius of the Saturnian core. If the core radius is $0.2R_s$, $0.219R_s$ and $0.24R_s$, $\sim 10^{14}$ Pa s, $\sim 5 \times 10^{13}$ Pa s, and $\sim 2.5 \times 10^{13}$ Pa s of viscosities are required, respectively. In the case of these viscosity values, dissipation of Saturn is consistent with both the latest observational results and the Mimas' orbital evolution.

In this work, we assume that the solid core and the envelope are homogeneous, and that rigidity and viscosity of the core do not change with time. Detailed interior structure models of Saturn and thermal evolution models can constrain the dissipation mechanisms more precisely, which should be addressed in future studies.

Acknowledgements. This work was supported by a JSPS Research Fellowship.

References

- Anderson, J. D., & Schubert, G. 2007, *Science*, 317, 1384.
- Chandrasekhar, S. 1969, *Ellipsoidal Figures of Equilibrium*. The Silliman Foundation Lectures. (Yale Univ. Press)
- Charnoz, S., et al. 2011, *Icarus*, 216, 535
- Gavrilov, S. V., & Zharkov, V. N. 1977, *Icarus* 37, 443
- Giampieri, G., Dougherty, M. K., Smith, E. J. & Russell, C. T. 2006, *Nature*, 441, 62
- Goldreich, P., & Soter, S. 1966, *Icarus*, 5, 375
- Jacobson, R. A., et al. 2006, *AJ*, 132, 2520
- Lainey, V., et al. 2012, *ApJ*, 752:1
- Lainey, V., et al. 2017, *Icarus*, 281, 286
- Meyer, J., & Wisdom, J. 2007, *Icarus*, 188, 535
- Murray, C. D., & Dermott, S. F. 2000, *Solar system Dynamics* (Cambridge University Press)
- Porco, C. C., et al. 2006, *Science*, 311, 1393
- Remus, F., Mathis, S., Zahn, J. -P., & Lainey, V. 2012, *A&A*, 541, A165
- Remus, F., Mathis, S., Zahn, J. -P., & Lainey, V. 2015, *A&A*, 573, A23
- Thomas, P. C., et al. 2007, *Icarus*, 190, 573